European Polymer Journal 46 (2010) 1345–1354

Contents lists available at ScienceDirect

European Polymer Journal

journal homepage: www.elsevier.com/locate/europolj

Development of the mesomorphic phase in isotactic propene/higher α-olefin copolymers at intermediate comonomer content and its effect on properties

M.J. Polo-Corpa [a], R. Benavente [a], T. Velilla [b,c], R. Quijada [b,c], E. Pérez [a], M.L. Cerrada [a,*]

[a] Instituto de Ciencia y Tecnología de Polímeros (CSIC), Juan de la Cierva, 3. 28006 Madrid, Spain
[b] Centro para la Investigación Multidisciplinaria Avanzada en Ciencias de los Materiales (CIMAT), Santiago, Chile
[c] Departamento de Ingeniería Química, Facultad de Ciencias Físicas y Matemáticas, Universidad de Chile, Casilla 2777, Chile

ARTICLE INFO

Article history:
Received 4 December 2009
Received in revised form 3 February 2010
Accepted 15 March 2010
Available online 21 March 2010

Keywords:
Isotactic polypropylene
Propylene-α-olefin copolymers
Metallocene catalyst
Monoclinic crystallites
Mesomorphic phase

ABSTRACT

Several isotactic propene-α-olefin copolymers using 1-octene, 1-dodecene and 1-tetradecene as comonomers (CiPO, CiPDD and CiPTD, respectively) have been synthesized and their structure and thermal/mechanical/viscoelastic properties have been evaluated. At intermediate comonomer molar content ranged from around 4 to 9, the mesomorphic phase is developed under rather mild quenching conditions and independently of length of the comonomer. Thermal and mechanical parameters diminish as α-olefin content increases and their dependence on composition changes as function of existence of three-dimensional monoclinic crystallites or less ordered entities.

1. Introduction

Isotactic polypropylene, iPP, exhibits an interesting polymorphic behavior, depending on microstructural features, crystallization conditions and other factors like the use of specific nucleants. Thus, three different polymorphic modifications, α, β and γ, all sharing a three-fold conformation [1–4], have been reported. In addition, fast quenching of iPP leads to a phase of intermediate or mesomorphic order [1,4–7].

The monoclinic α form is the most common and stable modification [8], being found in all kinds of solution-crystallized iPP samples and also in most melt-crystallized specimens [1,2,4,8,9]. The trigonal β modification [10,11] is a metastable phase and it is developed only under special crystallization conditions or in the presence of selective β nucleating agents [1–4,12–14]. The orthorhombic γ form [15] has been found in the case of low-molecular weight iPP and in random copolymers of propylene and α-olefins [1,2,4,11,16] or by the effect of pressure [17]. Moreover, the γ modification is especially favored in the case of iPP synthesized by metallocene catalysts, because of the presence of errors homogeneously distributed among the different polymer chains [18–23].

In addition to those four modifications, a new form has been recently reported [24–30] in the case of copolymers of iPP with medium and high contents of 1-hexene or 1-pentene as comonomers, crystallized at moderate rates and annealed at room temperature. The new modification, reported to have a trigonal unit cell [26,27,30], is the only one obtained for comonomer contents above around 14 mol.%, while variable proportions of it with the α modification were found in the comonomer range from around 8 to 13 mol.% in 1-hexene. However, it has been also reported that propylene-1-hexene and propylene-1-octadecene copolymers prepared by a relatively fast cooling from the molten state with comonomer molar contents ranging from 5 to 10 develop the aforementioned mesomorphic structure [31–33]. The formation of this phase of

* Corresponding author. Tel.: +34 915622900; fax: +34 915644853.
E-mail address: mlcerrada@ictp.csic.es (M.L. Cerrada).

0014-3057/$ - see front matter © 2010 Elsevier Ltd. All rights reserved.
doi:10.1016/j.eurpolymj.2010.03.014

intermediate order in these copolymers is much easier than that observed in either effective-quenched or stretched iPP [1,4,34,35].

It has been recently established [36] that the α crystals are not the only competitors of the trigonal form in an iPP-1-hexene copolymer with 8.6 mol.% content but the mesomorphic phase is also a key player.

The aims of this investigation are, on one hand, to learn if the arrangement in the mesomorphic form is a general event in fast cooled propylene copolymers synthesized by an isospecific metallocene catalyst with medium comonomer contents, independently of the comonomer type incorporated, and, on the other hand, to know how length of the lateral chain branching affects thermal and mechanical parameters. To reach these two main goals metallocene copolymers of propylene with 1-octene, 1-dodecene and 1-tetradecene with different comonomer contents have been synthesized and compared with those obtained previously using 1-hexene and 1-octadecene as comonomers at a given composition. The structural and thermal characterization has been carried out by wide-angle X-ray diffraction experiments and calorimetric analyses, whereas the evaluation of the viscoelastic behavior has been performed by dynamic-mechanical thermal analysis, and the mechanical response, using uniaxial tensile stress–strain measurements.

2. Experimental part

Copolymerization of propylene with the different high α-olefins considered (1-octene, 1-docedene and 1-tetradecene) was performed as described elsewhere [37] with toluene as a solvent in a Slurry system in 1 L Buchi glass reactor, using the rac-$Me_2Si(2\text{-}Me\text{-}Ind)_2ZrCl_2$/MAO catalytic system. The results about either comonomer in the different samples analyzed, determined by ^{13}C NMR spectroscopy, are shown in Table 1. The different copolymers were labeled as CiPO, CiPDD and CiPTD for 1-octene 1-dodecene and 1-tetradecene comonomer units, respectively, followed by a number that specifies their comonomer molar contents. The copolymers [33] with 1-hexene and 1-octadecene used as comparison at a given composition were named CiPH and CiPOD, respectively. A sample of iPP homopolymer was also prepared under the same conditions.

Table 1
NMR and GPC characterization of the different propylene copolymers.

Sample	Type of comonomer	Comonomer content (mol.%)	Comonomer content (wt.%)	M_w (kg/mol)
iPP	–	–	–	224
CiPO2.2	1-Octene	2.2	5.7	142
CiPO5.6	1-Octene	5.6	13.7	135
CiPO7.2	1-Octene	7.2	17.1	118
CiPDD4.6	1-Dodecene	4.6	16.2	163
CiPDD9.3	1-Dodecene	9.3	29.1	151
CiPTD2.0	1-Tetradecene	2.0	8.7	150
CiPTD4.7	1-Tetradecene	4.7	18.7	134
CiPH4.6	1-Hexene	4.6	8.8	120
CiPOD5.3	1-Octadecene	5.3	25.1	206

The molecular weights were determined by gel permeation chromatography in a Waters 150 CV-plus system equipped with an optical differential refractometer (model 150 C). A set of three columns of the Styragel HT type (HT3, HT4, and HT6) was used with 1,2,4-trichlorobenzene as a solvent. Standards of polystyrene and polyethylene with narrow molecular mass distribution were used for calibration.

Sheets of each polymer were prepared by compression molding between hot plates at a temperature about 20 °C above the melting point in a Collin press at a pressure of around 20 bar for 3 min. The samples were rapidly cooled from the molten state to room temperature between water plates at the same pressure. The thickness of the different films ranged from 0.2 to 0.3 mm.

Wide-angle X-ray diffraction (WAXD) patterns were recorded in the reflection mode at room temperature by using a Philips diffractometer with a Geiger counter, connected to a computer. Ni-filtered CuK_α radiation was used. The diffraction scans were collected over a period of 20 min in the range of 2θ values from 3° to 43°. The goniometer was calibrated with a silicon standard. The WAXD degree of crystallinity, f_c^{WAXD}, was determined from the X-ray diffractograms after subtraction of the amorphous profile [38].

Synchrotron experiments at wide angle were performed on the Non-Crystalline Diffraction Station of the Spanish Collaborative Research Group (CRG) beamline BM16-CRG at the ESRF (Grenoble, France). X-ray photographs were acquired using a MarCCD 165 detector (in 1024 × 1024 pixels mode) located at 250 mm from the polymer sample. The X-ray beam was monochromatized at the Selenium K-edge energy ($\lambda = 0.0978$ nm). The 2D X-ray diffractograms were processed using the FIT2D program of Dr. A. Hammersley of ESRF (http://www.esrf.fr/computing/scientific/FIT2D). The profiles were normalized to the primary beam intensity and the background from an empty sample was subtracted. The corresponding profiles represent relative intensity units as a function of the scattering vector, $q = 2\pi/d = 4\pi(\sin\theta)/\lambda$.

The synchrotron studies at small angle were performed in the Soft-Condensed Matter beamline A2 at Hasylab (Hamburg, Germany), working at a wavelength of 0.150 nm. The experiments were carried out at room temperature and a MarCCD detector was used for acquiring SAXS patterns (sample-to-detector distance being 260 cm). The different orders of the long spacing of rat-tail ($L = 65$ nm) were utilized for the SAXS detector calibration.

Calorimetric analyses were carried out in a TA Instruments Q100 calorimeter connected to a cooling system and calibrated with different standards. The sample weights ranged from 6 to 9 mg and the heating rate used was 20 °C min^{-1}. For crystallinity determinations, a value of 209 J g^{-1} has been taken as enthalpy of fusion of a perfect crystalline material [39].

Dynamic mechanical relaxations were measured with a Polymer Laboratories MK II Dynamics Mechanical Thermal Analyzer, working in a tensile mode. The storage modulus, E', loss modulus, E'', and the loss tangent, tan δ, of each sample were obtained as function of temperature over

the range from –150 to 150 °C at fixed frequencies of 1, 3, 10, 30 Hz, and at a heating rate of 1.5 °C/min. Strips of 2.2 mm wide and 15 mm length were cut from the molded sheets.

Stress–strain measurements were performed using an Instron dynamometer equipped with a load cell and an integrated digital display that provided force determinations. Dumbbell samples with an effective length of 15 mm and a width of 1.9 mm were cut from the compression-molded sheets. These specimens were then stretched at a strain rate of 10 mm/min at 23 °C, and Young's modulus (E), yield stress (σ_Y) and strain (ε_Y) and stress and strain at break (σ_B and ε_B) were determined. The Young's modulus was measured from the slope of the curve at very small deformations (the initial linear part of the curve). On the other hand, the yield stress and strain values were usually calculated from the maximum on the stress–strain curves obtained. If a maximum was not observed, the yield point was estimated by the tangent method. The values reported for Young's modulus, yield stress and strain are averages from, at least, three different specimens of each sample.

3. Results and discussion

3.1. Structural and thermal properties

Table 1 shows the main characteristics of the propylene copolymers synthesized with the different comonomeric units. It is noteworthy that the values of the molecular weight are rather similar for all of these copolymers and, moreover, no significant differences are expected in the content of stereo and regio-regularity defects because of the synthetic method used [33]. Therefore, these variables will not be relevant for explanation of the different variations in the copolymer structure and properties.

On the other hand, Fig. 1 shows the WAXD profiles at room temperature for the different copolymers and that found in the iPP homopolymer for comparison. It has to be reminded that all these specimens have been rapidly cooled under compression molding. It can be observed that the profiles of the neat iPP and CiPO2.2 and CiPTD2.0 copolymers exhibit the main diffractions characteristic of the α monoclinic iPP crystalline modification [7,40]. In addition, it is noticeable that no evidence of the γ modification is observed, most probably because of the relatively high cooling rate used during processing of these copolymers. The intensity of the different reflections decreases and, consequently, crystallinity becomes smaller as comonomer is incorporated (see also Table 2). Moreover, a broadening of diffractions and a shift of their location to lower angles are also evident if compared with the iPP profile. These two features are related to the existence of thinner ordered entities as comonomer content is raised in the copolymer. This assumption can be confirmed by determination of the long spacing at room temperature of these ordered entities by SAXS. For instance, Fig. 2 shows the SAXS profiles for the homopolymer and the copolymers with 1-octene. From these maxima, the long spacings, L^{SAXS}, have been determined, and are listed in Table 2. With these values and the total WAXD crystallinity of the sample, f_c^{WAXD},

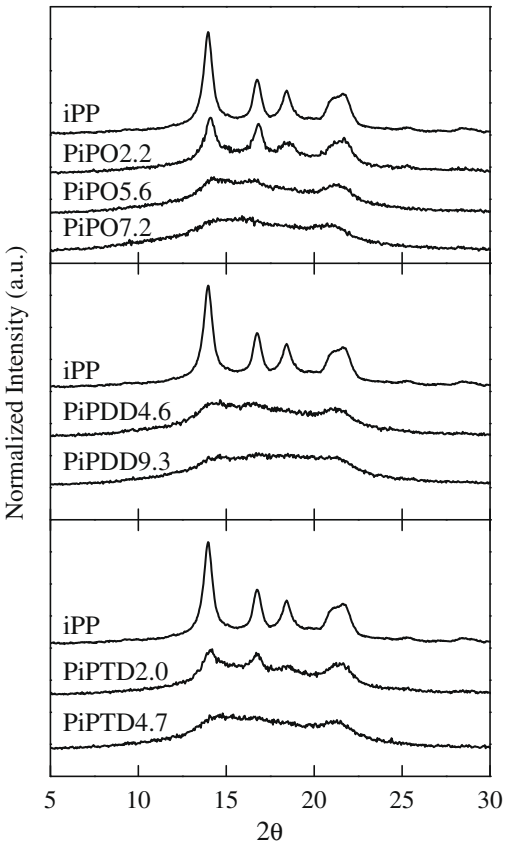

Fig. 1. X-ray diffraction patterns, at room temperature, in rapidly cooled and compressed-molded specimens of iPP and the different copolymers analyzed: CiPO, CiPDD and CiPTD from top to bottom plots, respectively.

the most probable crystallite size in the direction normal to the lamellae, l_c, can be determined by assuming a simple two-phase model, i.e. $l_c = f_c^{WAXD} \times L^{SAXS}$. The results for l_c are also listed in Table 2. On one hand, long spacing is observed in all of the specimens and, on the other hand, the higher comonomer content is the smaller size of ordered entities becomes.

The profiles exhibited by the copolymers with molar content of around 5% under study – CiPO5.6, CiPDD4.6 and CiPTD4.7 – and those taken from literature, CiPH4.6

Table 2
Overall degree of crystallinity, f_c, (obtained by WAXD), content of monoclinic crystallites, f_α^{WAXD}, long spacing, L^{SAXS}, and most probable size of ordered entities, l_c, determined at room temperature.

Sample	f_c^{WAXD}	f_α^{WAXD}	L^{SAXS} (nm)	l_c (nm)
iPP	0.60	0.60	11.8	7.1
CiPO2.2	0.40	0.40	9.3	3.7
CiPO5.6	0.22	0.07	9.0	2.0
CiPO7.2	0.16	0.02	10.1	1.6
CiPDD4.6	0.22	0.06	8.7	1.9
CiPDD9.3	0.15	0.00	11.1	1.7
CiPTD2.0	0.27	0.27	9.3	2.5
CiPTD4.7	0.18	0.03	9.2	1.7
CiPH4.6	0.20	0.08	–	–
CiPOD5.3	0.24	0.00	–	–

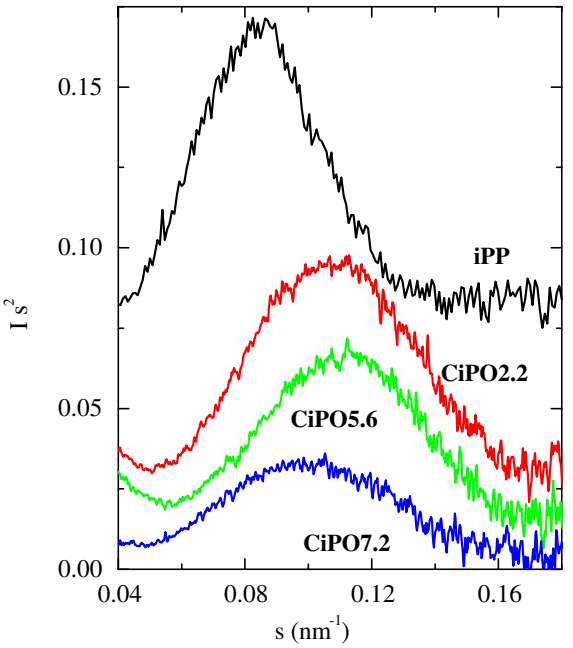

Fig. 2. Lorentz-corrected SAXS profiles, at ambient temperature, for the iPP homopolymer and the different 1-octene copolymers. From top to bottom: iPP, CiPO2.2, CiPO5.3 and CiPO7.2.

and CiPOD5.3 for comparative reasons [33], are depicted in Fig. 3. The coexistence of very imperfect α crystals and the mesomorphic modification seems to take place simultaneously at these intermediate contents. However, if comonomer molar content is further increased the mesomorphic form is the only observed, as seen in Fig. 1 and in agreement with literature data [32,33]. This mesomorphic profile is, evidently, somewhat different to that found for iPP homopolymer [41] due to the fact that now in these CiPO7.2 and CiPDD9.6 samples, with around 17 and 32 wt.% comonomer content, the non-crystalline profile is expected to have an important contribution at around 19–20°, arising from the comonomer. Another interesting difference with iPP homopolymers is the experimental conditions at which this mesomorphic form is developed. The mesomorphic phase in iPP homopolymer is obtained under very fast quenching conditions [1–4] and from the stretching of the γ polymorph [23,42,43] in metallocene iPP. However, the cooling conditions are getting milder when either content increases for a given copolymer type or comonomer length is enlarged at an almost constant molar content. Thus, Fig. 1 indicates that copolymers CiPO7.2 and CiPDD9.6, as also observed in CiPH8.6 and CiPOD7.6 copolymers [33,36], lead almost to the pure mesomorphic modification by cooling in the press with refrigerating water, while the homopolymer and the other copolymers with smaller comonomer content lead to the α polymorph. Fig. 4 depicts the content of the α polymorph, f_α^{WAXD}, deduced from the diffractograms.

Therefore, (a) at low contents, around 2 mol.%, the ordered entities that exist are exclusively α crystallites – no presence of γ polymorph is detected because of the fast cooling rate applied; (b) coexistence of α crystals and the mesomorphic form is observed at intermediate contents, the proportion of the former diminishing as comonomer length increases, and (c) at higher contents, around 8–9 mol.%, the mesomorphic form is the only one developed (see Table 2).

Fig. 5 shows the DSC curves corresponding to the first melting process exhibited by the different samples. As observed, T_m values are significantly shifted to lower temperatures as comonomer content is increased (see results in

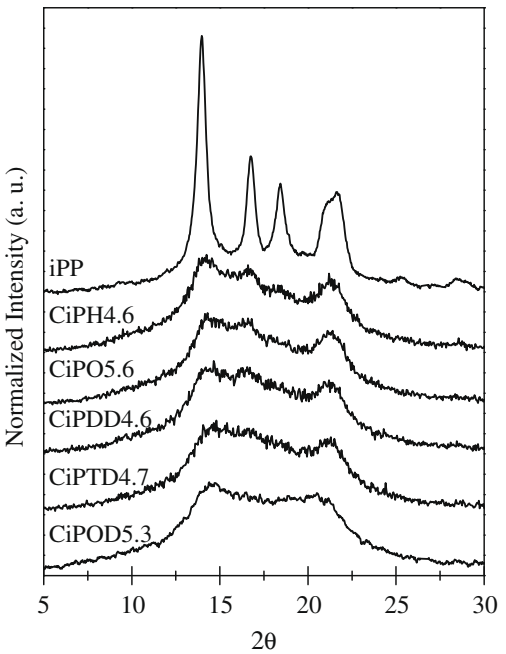

Fig. 3. X-ray diffraction patterns, at room temperature, in rapidly cooled and compressed-molded specimens of different copolymers with similar comonomeric content. Those profiles related to 1-hexene and 1-octadecene have been taken from literature to establish a complete comparison.

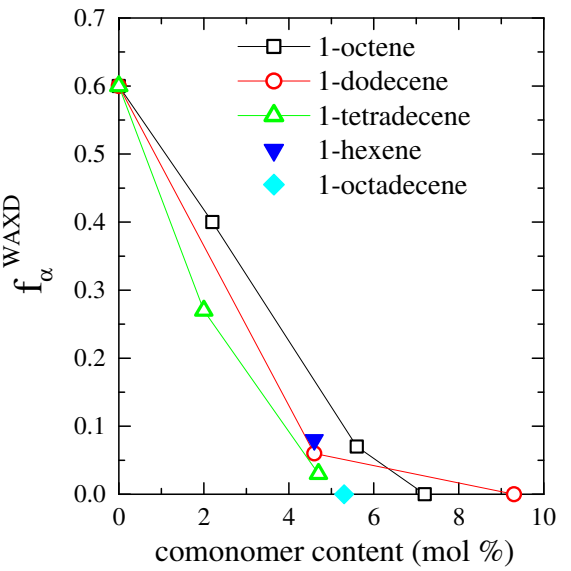

Fig. 4. Dependence of α crystallites content on comonomer content for the different copolymers under study. Values found in CiPH4.6 and CiPOD5.3 copolymers are also included.

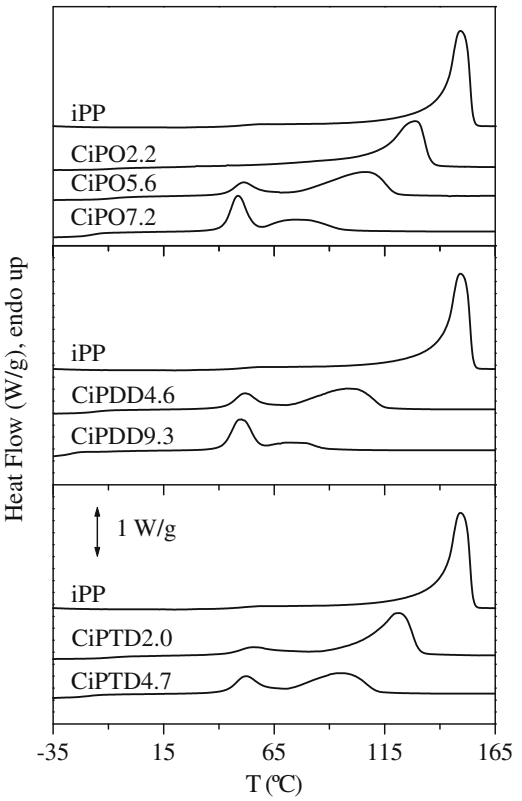

Fig. 5. DSC first melting curves performed at 20 °C min^{-1} in the iPP homopolymer and in the CiPO (top plot), CiPDD (middle plot) and CiPTD (bottom plot) copolymers.

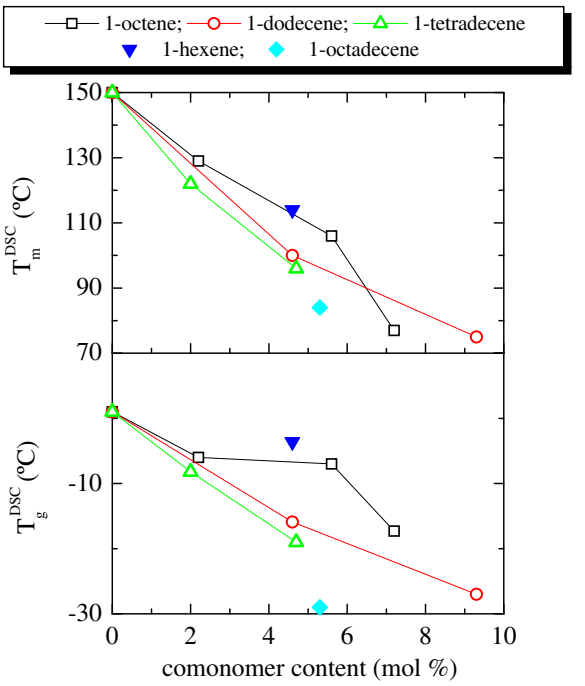

Fig. 6. Dependence of melting temperature, T_m, (upper plot) and glass transition temperature, T_g, (lower plot) on comonomer content for the different copolymers, determined both temperatures from the first melting process performed at 20 °C min^{-1}.

Table 3 and upper plot of Fig. 6). The same decreasing trend is found for crystallization temperatures. The non-inclusion of comonomer units within crystallites reduces the length of the main chain able to crystallize as comonomer content increases and, consequently, crystal thickness decreases, crystal lattice is substantially distorted, as aforementioned, and overall crystallinity is lowered, as deduced from results listed in Table 3.

In addition, a clear endothermic peak at around 50 °C is observed in the different quenched samples and its intensity increases as comonomer content does, becoming the most prominent peak of the curve in the copolymers with the highest contents, i.e. CiPO7.2 and CiPDD9.3. This peak has been traditionally assigned to the melting of those crystals reorganized during the long time annealing at room temperature. There is an important fraction of the sample that has crystallized into rather small and imperfect α crystallites because of the fast cooling applied during processing. Therefore, these crystalline entities are able to melt and recrystallize during the stay of samples at room temperature prior to their analysis and, consequently, the initial small α crystallites are slightly enlarged, leading to the appearance of that peak located at 40–50 °C, which is present even in the neat iPP. This hypothesis is valid for the homopolymer and copolymers with low comonomer contents. However, it is well known that in mesomorphic iPP homopolymer [7] there is a crystal-like (mesomorphic phase) to crystal (α crystallites) phase transition, which presumably may also occur in the present samples. In fact, it has been reported for a propylene-1-hexene copolymer with a molar fraction of 8.7 that a melting-recrystallization process from the mesomorphic entities to the α crystals takes place at around 50 °C, as deduced from real-time X-ray measurements [36].

Consequently, real-time experiments, employing synchrotron radiation, have been performed on sample CiPO7.2 and the results are shown in Fig. 7. These diffractograms exhibit very good signal-to-noise ratio, and a certain amount of α crystals is present in the initial sample, although it is mostly mesomorphic. With increasing temperature, and at around 60 °C, the transformation mesomorphic to α form is observed, these α crystals melting

Table 3
DSC values for the different thermal transitions existing in the first melting process: glass transition, T_g, and melting, T_m, temperatures. Crystallization temperature during cooling, T_c, is also reported. The DSC crystallinity, f_c^{DSC}, is also evaluated in the first melting.

Sample	T_g (°C)	T_m (°C)	T_c (°C)	f_c^{DSC}
iPP	1	150	104	0.48
CiPO2.2	−6	129	85	0.34
CiPO5.6	−7	107	45	0.27
CiPO7.2	−17	77	5	0.20
CiPDD4.6	−16	100	44	0.25
CiPDD9.3	−27	75	−1	0.16
CiPTD2.0	−8	122	75	0.33
CiPTD4.7	−19	96	42	0.24
CiPH4.6	−4	114	56	0.30
CiPOD5.3	−29	84	17	0.24

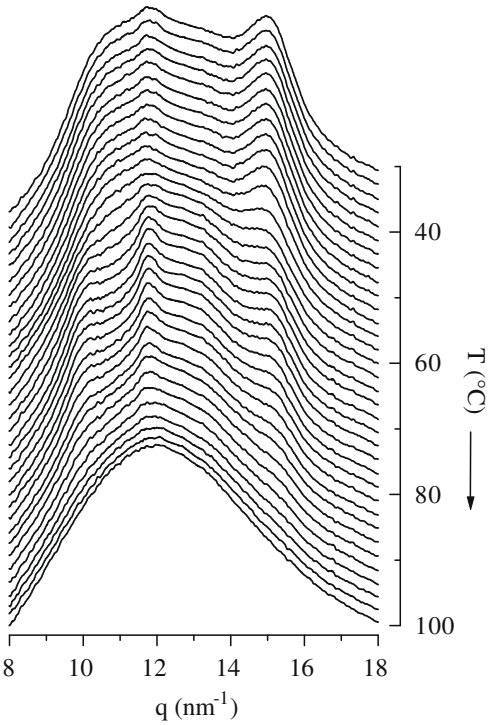

Fig. 7. Real-time variable-temperature diffractograms corresponding to a melting experiment, at 8 °C min^{-1}, for sample CiPO7.2.

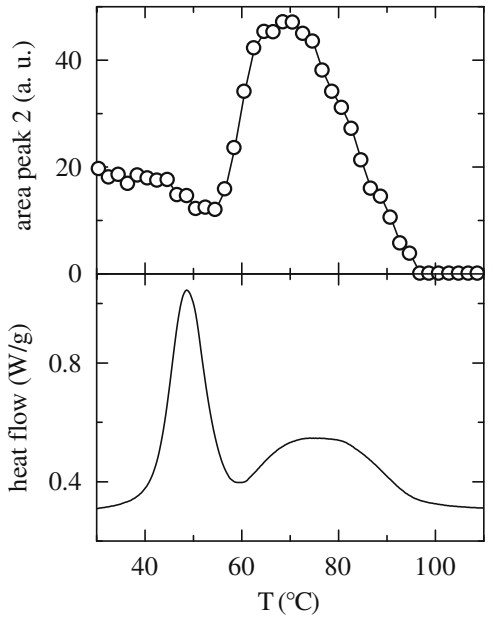

Fig. 8. Temperature dependence of the intensity (upper plot) of the diffraction located at q around 11.7 nm^{-1} in Fig. 6, compared with the DSC heating curve (lower plot).

finally at around 95 °C. These transformations can be monitored from the intensity of the peak at q around 11.7 nm^{-1} (corresponding to 2θ around 16.5° for CuK_α radiation, as in Fig. 1). The variation with temperature of the area of that peak is shown in the upper part of Fig. 8 compared with the DSC melting curve (lower plot of Fig. 8). It is important to note that the recrystallization of the mesomorphic phase into the α crystals is not inferred from the DSC melting curve, since it does not go below the baseline (exothermic). However, a process is clearly observed from the synchrotron results, being centered at around 60 °C. Moreover, there seems to be an initial decrease of the α peak intensity up to 55 °C, so that the first melting peak can be assigned both to the melting of some initial, rather imperfect, α crystals plus to the melting-recrystallization process of the mesomorphic entities into α crystallites.

Anyway, from these experiments and from the results in Fig. 1, it can be anticipated that in all these copolymers, when the comonomer content is higher than around 4–5 mol.%, the majority of the ordered entities are of the mesomorphic type, which will undergo, on heating, a transformation into α crystals, prior to the final melting.

Coming back to the DSC heating curves in Fig. 5, another very interesting feature is the behavior of the glass transition. A significant variation of T_g is observed with both the comonomer content and the type of comonomer, as depicted in lower plot of Fig. 6 for the initial melting. It seems clear that the depression of the glass transition is deeper as either composition or length of comonomer increase in the copolymer. Thus, a reduction of around 30 °C is observed in the case of the copolymer CiPDD9.3, although it has to be considered that this sample incorporates a 29% by weight of 1-dodecene comonomer. In relation with the type of chain branching, it is clearly seen that mobility within the amorphous regions is considerably much higher as length in comonomeric unit is increased when comparing the different comonomers at a composition of around 5 mol.% (see Fig. 6).

3.2. Dynamic-mechanical response

Fig. 9 represents the DMTA curves for polypropylene and the CiPTD copolymers as function of temperature. Several relaxation processes are observed in plots of loss magnitudes, tan δ and E'', for these copolymers. These relaxations are also found in the copolymers with 1-octene and 1-dodecene, as seen in Fig. 10 for tan δ, and. reported in Table 4. The relaxation at the highest temperature, named as α, is related to motions within the polymer crystalline phase, especially to defect diffusion [44]. As the comonomer content increases, its location is shifted to lower temperatures, as seen from the E' and E'' plots, because of the reduction in crystallinity and crystal size, as previously discussed. It has been described that changes in the amorphous phase can also explain the behavior of this relaxation in copolymers, due to the drifts in properties of the interphase, helping to relax the diffusion of ending defects in that region [44].

The relaxation placed at around 0 °C is ascribed to generalized motions of long chain segments that take place along the glass transition. The cooperative nature of this movement explains the great decrease in E' found in this temperature range. Its intensity in tan δ rises as comonomer content does in the copolymer because of the increase in the amorphous fraction within the polymeric material.

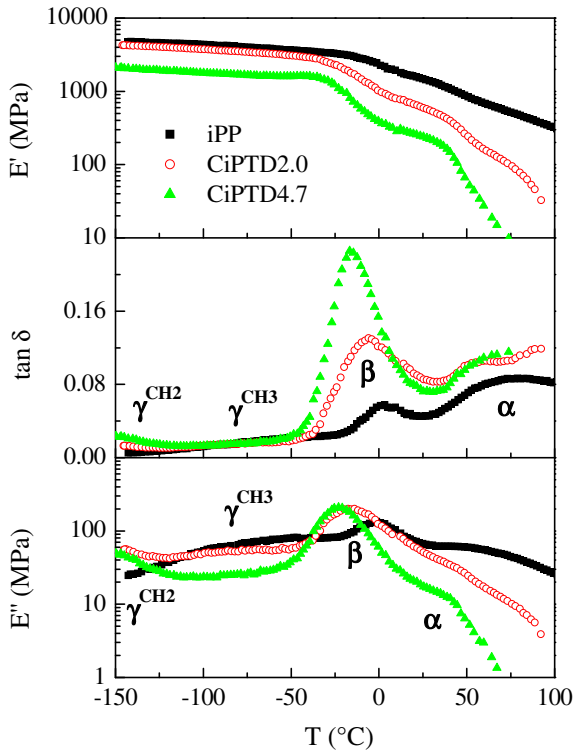

Fig. 9. Variation of the storage modulus (E'), tan δ and loss modulus (E'') with temperature, at 3 Hz, for iPP and the CiPTD copolymers.

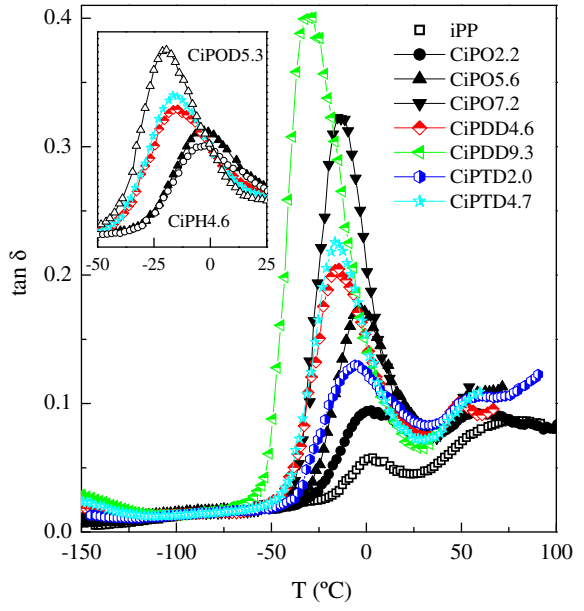

Fig. 10. Variation of tan δ with temperature, at 3 Hz, for iPP and the distinct propylene copolymers. In the inset, copolymers at molar content around 5% are compared; CiPH4.6 and CiPOD5.3 are also included.

Accordingly, the location of the β relaxation also changes with composition, shifting down to lower temperatures with increasing comonomer content, because of hindrance reduction as the amount of ordered entities diminishes. At approximately constant comonomer content, in agreement with the T_g calorimetric values, the β relaxation takes place at lower temperatures and its intensity is enlarged as length of branching increases, as clearly depicted in the inset of Fig. 10 for CiPH4.6, CiPO5.6, CiPDD4.6, CiPTD4.7 and CiPOD5.3 copolymers. This fact is associated, on one hand, with the higher flexibility of lateral chains and, on the other hand, with the larger free volume caused by the longer comonomeric unit.

Table 4
Location of relaxation processes on tan δ basis at 3 Hz for the different specimens under study.

Sample	T_α (°C)	T_β (°C)	T_γ^{CH3} (°C)	T_γ^{CH2} (°C)
iPP	80	2	−42	–
CiPO2.2	57	3	−62	–
CiPO5.6	55	−3	−77	−148
CiPO7.2	–	−13	−86	−148
CiPDD4.6	47	−15	−81	−150
CiPDD9.3	–	−30	−85	−150
CiPTD2.0	58	−6	−68	−144
CiPTD4.7	51	−17	−80	−148
CiPH4.6	57	−3	−77	–
CiPOD5.3	–	−20	−58	−149

Other relaxation process, labeled as γ^{CH3}, ascribed to rotational motions of methyl groups from polypropylene, is observed at temperatures slightly lower than that related to cooperative motions. It does actually appear as a shoulder and not as a well-defined peak in even in the iPP homopolymer (see Fig. 9). In addition to this γ^{CH3} mechanism, the copolymers with relatively high comonomer contents, independently of the type, show an extra relaxation [31,45] named as γ^{CH2}, at around −150 °C. This new process seems to have the same molecular cause than the γ-relaxation [31,46,47] in polyethylene, which requires, at least, three or more consecutive methylene units. Therefore, the more methylene units are the more intense this relaxation is.

Fig. 9 also depicts the dependence of E', related to the elastic contribution to the complex modulus, on comonomeric incorporation. Values are reduced from homopolymer to the copolymers, this decrease being more significant as comonomer composition is raised. Monoclinic crystallites are the stiffer component and their amount and size are lowered as α-olefin content increases.

3.3. Stress–strain

Fig. 11 shows the results from stress–strain tests for the different copolymers. Great changes are observed in the main mechanical parameters when the comonomer content varies, ascribed to the structural changes that take place. The most relevant variations are observed in the yield point and in the elastic modulus values, as seen in Table 5. The former becomes diffuse and the latest is reduced as comonomer content increases, indicating the transition from the necking deformation process typically exhibited by thermoplastic polymers to a ductile and elastomeric-like mechanism [31,48,49]. In addition, the decrease of α-crystal content and the appearance of a

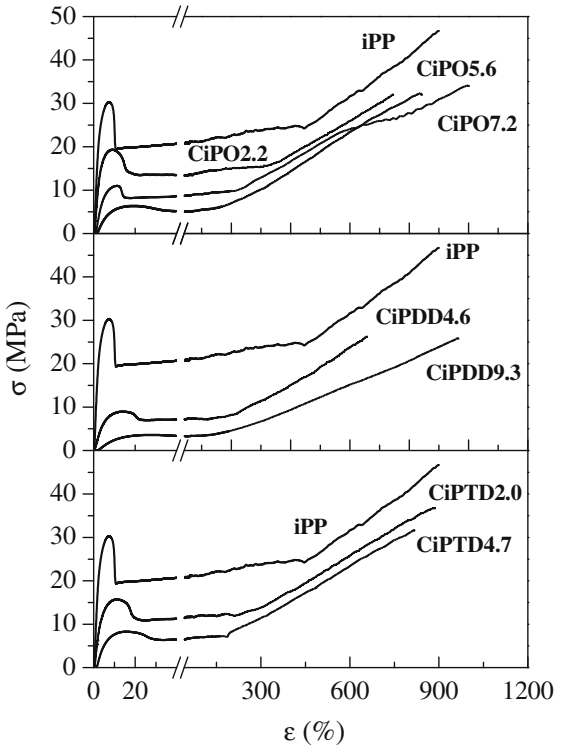

Fig. 11. Stress–strain curves for the iPP and the different CiPO, CiPDD and CiPTD copolymers.

Table 5
Main mechanical parameters obtained from nominal stress–strain measurements for the different propylene copolymers.

Sample	E (MPa)	σ_Y (MPa)	ε_Y (% ε)
iPP	1100	29	7
CiPO2.2	476	16	9
CiPO5.6	277	11	12
CiPO7.2	101	6	20
CiPDD4.6	173	9	13
CiPDD9.3	37	4	25
CiPTD2.0	421	14	11
CiPTD4.7	171	8	14
CiPH4.6	352	13	11
CiPOD5.3	92	6	15

softer mesomorphic form lead to a subsequent increase of flexibility as comonomer content is enlarged. The amorphous phase behaves as a viscoelastic liquid with low stress resistance compared with that exhibited by the ordered phase. Therefore, as ordering is reduced the content of amorphous regions is enlarged and, consequently, the stress resistance is lowered and the capability of being deformed significantly enlarged.

A high mobility is found, as aforementioned, in the amorphous regions of the copolymers as comonomer length increases, and then mechanical parameters obtained from the stress–strain curves consequently change depending on content and type of chain branching. Thus, focusing the attention in Table 5 at the copolymers with around 5 mol.% comonomer content, both the Young's modulus and the stress at yield seem to decrease with the increase in the branch length, which seems to be connected with the fact that the mesomorphic phase ease of formation follows also the same trend.

The decrease of the elastic modulus and yield stress with increasing comonomer concentration and, therefore, lowering crystallinity here commented has been also found in some other ethylene or hexene copolymers [28,50] whereas a different response is observed for copolymers with 1-butene as comonomeric unit, then the Young's modulus being nearly constant with changing 1-butene composition [28].

4. Conclusions

A considerable decrease in crystallinity is observed with comonomer content in these quenched copolymers. Moreover, the crystal lattice varies from a monoclinic cell at low contents to mesomorphic-like ordered entities for the highest ones. These variations in crystal structure significantly influence the location of thermal transitions as well as the viscoelastic and mechanical behavior of these copolymers.

Several relaxation processes take place, their location and intensity being strongly dependent upon composition. As comonomer content increases, the intensity of α relaxation, ascribed to motions within crystalline regions, diminishes and that related to the process associated with cooperative movements within amorphous phase (β relaxation) increases. Moreover, a shift of their location to lower temperatures is also observed for both processes. On the other hand, a relaxation related to internal motions within the comonomeric units (labeled as γ^{CH2}) is seen in the range of very low temperatures as CH_2 content is high enough to be this movement detected. This process is ascribed to movements of methylenic segments within the comonomer and, consequently, is strongly dependent on composition and length of incorporated units.

The cold-drawing deformation mechanism characteristic for iPP evolves to another rather homogeneous-like simply varying the composition when deformation takes place at room temperature. Rigidity strongly diminishes and toughness (estimated from integration of stress–strain curves) increases with comonomer content, these changes being more significant as comonomer length increases and α crystallites are transformed into mesomorphic entities.

These results, joined to some others previously reported for copolymers of propylene with 1-hexene and 1-octadecene, point out that a mesomorphic ordering is developed in propylene copolymers at not very fast cooling rates.

Acknowledgements

The authors are grateful for the financial supports of Ministerio de Educación y Ciencia (project MAT2007-65519-C02-01) and CONICYT (project FONDAP 11980002). We also thank to Dr. G. Galland her help in the ^{13}C NMR analysis performed for the different specimens. The synchrotron work at ESRF was also supported by MEC through specific grants for the access to the CRG beamline BM16 of the ESRF. The synchrotron work at Hasylab was supported by the European Community – Research Infrastructure

Action under the FP6 "Structuring the European Research Area" Programme (through the Integrated Infrastructure Initiative "Integrating Activity on Synchrotron and Free Electron Laser Science"), contract RII3-CT-2004-506008 (IA-SFS). The inestimable help of all the personnel of the two beamlines is also gratefully acknowledged.

References

[1] Brückner S, Meille SV, Petraccone V, Pirozzi B. Polymorphism in isotactic polypropylene. Prog Polym Sci 1991;16:361–404.
[2] Lotz B, Wittmann JC, Lovinger AJ. Structure and morphology of poly(propylenes): a molecular analysis. Polymer 1996;37:4979–92.
[3] Varga J. Supermolecular structure of isotactic polypropylene. J Mater Sci 1992;27:2557–79.
[4] Phillips PJ, Mezghani K. In: Salamone JC, editor. The polymeric materials encyclopedia, vol. 9. Boca Raton: CRC Press; 1996. p. 6637.
[5] Slichter WP, Mandell ER. Molecular motion in polypropylene, isotactic and atactic. J Appl Phys 1958;29:1438–41.
[6] Corradini P, de Rosa C, Guerra G, Petraccone V. Comments on the possibility that the mesomorphic form of isotactic polypropylene is composed of small crystals of the beta-crystalline form. Polym Commun 1989;30:281–5.
[7] Arranz-Andrés J, Benavente R, Pérez E, Cerrada ML. Structure and mechanical behavior of the mesomorphic form in a propylene-b-EPR copolymer and its comparison with other thermal treatments. Polym J 2003;35:766–77.
[8] Natta G, Corradini P. Structure and properties of isotactic polypropylene. Nuovo Cimento Suppl 1960;15:40–51.
[9] Jones AT, Aizlewood JM, Beckett DR. Crystalline forms of isotactic polypropylene. Makromol Chem 1964;75:134–58.
[10] Meille SV, Ferro D, Brückner S, Lovinger AJ, Padden FJ. Structure of beta-isotactic polypropylene – a long-standing structural puzzle. Macromolecules 1994;27:2615–22.
[11] Lotz B, Kopp S, Dorset DC. Original crystal structure of polymers with ternary helixes. R Acad Sci Paris Ser IIb 1994;319:187–92.
[12] Keith HD, Padden FJ, Walter NM, Wyckoff HW. Evidence for a second crystal form of polypropylene. J Appl Phys 1959;30:1485–8.
[13] (a) Varga J. In: Karger-Kocsis J, editor. Polypropylene: structure, blends and composites, vol. 1. London: Chapman and Hall; 1995. p. 56;
(b) Varga J. Supermolecular structure of isotactic polypropylene. J Macromol Sci Phys B 2002;41:1121–71;
(c) Varga J, Ehrenstein W. In: Karger-Kocsis J, editor. Polypropylene: an A–Z reference. London: Kluwer; 1999. p. 51.
[14] Krache R, Benavente R, López-Majada JM, Pereña JM, Cerrada ML, Pérez E. Competition between alpha, beta and gamma polymorphs in a beta-nucleated metallocene isotactic polypropylene. Macromolecules 2007;40:6871–8.
[15] Brückner S, Meille SV. Non-parallel chains in crystalline gamma-isotactic polypropylene. Nature 1989;340:455–7.
[16] Addink EJ, Beintema J. Polymorphism of crystalline polypropylene. Polymer 1961;2:185–93.
[17] (a) Bruckner S, Phillips PJ, Mezghani K, Meille SV. On the crystallization of gamma-isotactic polypropylene: a high pressure study. Macromol Rapid Commun 1997;18:1–7;
(b) Mezghani K, Phillips PJ. The gamma-phase of high molecular weight isotactic polypropylene. 2. The morphology of the gamma-form crystallized at 200 Mpa. Polymer 1997;38:5725–33;
(c) Mezghani K, Phillips PJ. The gamma-phase of high molecular weight isotactic polypropylene: III. The equilibrium melting point and the phase diagram. Polymer 1998;39:3735;
(d) Dimeska A, Phillips PJ. High pressure crystallization of random propylene–ethylene copolymers: alpha-gamma phase diagram. Polymer 2006;47:5445.
[18] Pérez E, Zucchi D, Sacchi MC, Forlini F, Bello A. Obtaining the gamma phase in isotactic polypropylene: effect of catalyst system and crystallization conditions. Polymer 1999;40:675–81.
[19] Hosier IL, Alamo RG, Esteso P, Isasi JR, Mandelkern L. Formation of the alpha and gamma polymorphs in random metallocene–propylene copolymers. Effect of concentration and type of comonomer. Macromolecules 2003;36:5623–36.
[20] De Rosa C, Aurienma F, Paolillo M, Resconi L, Camurati I. Crystallization behavior and mechanical properties of regiodefective, highly stereoregular isotactic polypropylene: effect of regiodefects versus stereodefects and influence of the molecular mass. Macromolecules 2005;38:9143–54.
[21] Alamo RG, Kim M-H, Galante MJ, Isasi JR, Mandelkern L. Structural and kinetic factors governing the formation of the γ polymorph of isotactic polypropylene. Macromolecules 1999;32:4050–64.
[22] Aurienma F, De Rosa C. Crystallization of metallocene-made isotactic polypropylene: disordered modifications intermediate between the α and γ forms. Macromolecules 2002;35:9057–68.
[23] De Rosa C, Auriemma F, Di Capua A, Resconi L, Guidotti S, Camurati I, et al. Structure–property correlations in polypropylene from metallocene catalysts: stereodefective, regioregular isotactic polypropylene. J Am Chem Soc 2004;126:17040–9.
[24] Poon B, Rogunova M, Hiltner A, Baer E, Chum SP, Galeski A, et al. Structure and properties of homogeneous copolymers of propylene and 1-hexene. Macromolecules 2005;38:1232–43.
[25] Lotz B, Ruan J, Thierry A, Alfonso GC, Hiltner A, Baer E, et al. A structure of copolymers of propene and hexene isomorphous to isotactic poly(1-butene) form I. Macromolecules 2006;39:5777–81.
[26] De Rosa C, Dello Iacono S, Auriemma F, Ciaccia E, Resconi L. Crystal structure of isotactic propylene–hexene copolymers: the trigonal form of isotactic polypropylene. Macromolecules 2006;39:6098–109.
[27] De Rosa C, Auriemma F, Corradini P, Tarallo O, Dello Iacono S, Ciaccia E, et al. Crystal structure of the trigonal form of isotactic polypropylene as an example of density-driven polymer structure. J Am Chem Soc 2006;128:80–1.
[28] De Rosa C, Auriemma F, Ruiz de Ballesteros O, Resconi L, Camurati I. Tailoring the physical properties of isotactic polypropylene through incorporation of comonomers and the precise control of stereo and regioregularity by metallocene catalysts. Chem Mater 2007;19:5122–30.
[29] De Rosa C, Auriemma F, Ruiz de Ballesteros O, De Luca D, Resconi L. The double role of comonomers on the crystallization behavior of isotactic polypropylene: propylene–hexene copolymers. Macromolecules 2008;41:2172–7.
[30] De Rosa C, Auriemma F, Talarico G, Ruiz de Ballesteros O. Structure of isotactic propylene–pentene copolymers. Macromolecules 2007;40:8531–2.
[31] Palza H, López-Majada JM, Quijada R, Benavente R, Pérez E, Cerrada ML. Metallocenic copolymers of isotactic propylene and 1 octadecene: crystalline structure and mechanical behavior. Macromol Chem Phys 2005;206:1221–30.
[32] López-Majada JM, Palza H, Guevara JL, Quijada R, Martínez MC, Benavente R, et al. Metallocenic copolymers of propene and 1 hexene: influence of comonomer content and thermal history on the structure and mechanical properties. J Polym Sci Part B Polym Phys 2006;44:1253–67.
[33] Palza H, López-Majada JM, Quijada R, Pereña JM, Benavente R, Pérez E, et al. Comonomer length influence on the structure and mechanical response of metallocenic polypropylenic materials. Macromol Chem Phys 2008;209:2259–67.
[34] Androsch R, Wunderlich B. Reversible crystallization and melting at the lateral surface of isotactic polypropylene crystals. Macromolecules 2001;34:5950–60.
[35] Saraf RF. Planar and fiber textures induced in isotactic polypropylene on equibiaxial hydrostatic deformation. Polymer 1994;35:1359–68.
[36] Cerrada ML, Polo-Corpa MJ, Benavente R, Pérez E, Velilla T, Quijada R. Formation of the new trigonal polymorph in iPP-1-hexene copolymers. Competition with the mesomorphic phase. Macromolecules 2009;42:702.
[37] Quijada R, Guevara JL, Galland GB, Rabagliati FM, López-Majada JM. Synthesis and properties coming from the copolymerization of propene with alpha-olefins using different metallocene catalysts. Polymer 2005;46:1567–74.
[38] Mansel S, Pérez E, Benavente R, Pereña JM, Bello A, Roll W, et al. Synthesis and properties of elastomeric poly(propylene). Macromol Chem Phys 1999;200:1292–7.
[39] Wunderlich B. Macromolecular physics, vol. 3. New York: Academic Press; 1980. p. 42.
[40] Turner-Jones A. Development of the γ-crystal form in random copolymers of propylene and their analysis by DSC and X-ray methods. Polymer 1971;12:487–508.
[41] Konishi T, Nishida K, Kanaya T, Kaji K. Effect of isotacticity on formation of mesomorphic phase of isotactic polypropylene. Macromolecules 2005;38:8749–54.
[42] De Rosa C, Auriemma F, De Lucia G, Resconi L. From stiff plastic to elastic polypropylene: polymorphic transformations during plastic deformation of metallocene-made isotactic polypropylene. Polymer 2005;46:9461–75.
[43] De Rosa C, Auriemma F. Structural–mechanical phase diagram of isotactic polypropylene. J Am Chem Soc 2006;128:11024–5.

[44] Jourdan C, Cavaille JY, Perez J. Mechanical relaxations in polypropylene – a new experimental and theoretical approach. J Polym Sci Part B Polym Phys 1989;27:2361–84.
[45] Arranz-Andrés J, Guevara JL, Velilla T, Quijada R, Benavente R, Pérez E, et al. Syndiotactic polypropylene and its copolymers with alpha olefins. Effect of composition and length of comonomer. Polymer 2005;46:12287–97.
[46] Boyd RH, Breitling SM. Conformational-analysis of crankshaft motions in polyethylene. Macromolecules 1974;7:855–62.
[47] Heaton NJ, Benavente R, Pérez E, Bello A, Pereña JM. The gamma relaxation in polymers containing ether linkages: conformational dynamics in the amorphous phase for a series of polybibenzoates containing oxyethylene spacers. Polymer 1996;37:3791–8.
[48] Cerrada ML, Benavente R, Peña B, Pérez E. The effect of thermal treatment on the structure and relaxation processes of olefinic polymers synthesized with metallocene catalysts. Polymer 2000;41:5957–65.
[49] Benavente R, Pérez E, Quijada R. Effect of the comonomer content on the mechanical parameters and microhardness values in poly(ethylene-co-1-octadecene) synthesized by a metallocene catalyst. J Polym Sci Part B Polym Phys 2001;39:277–85.
[50] Arranz-Andrés J, Suárez I, Peña B, Benavente R, Pérez E, Cerrada ML. Metallocenic isotactic polypropylene and its copolymers with 1-hexene and ethylene: influence of comonomer content on the structure and mechanical properties. Macromol Chem Phys 2007;208:1510–21.